Macromolecules

pubs.acs.org/Macromolecules Article

Oligomer Content Determines the Properties and Application of Polycaprolactone

Caihong Gong, Yu Gu, Xi Wang,* and Chunwang Yi*

Cite This: *Macromolecules* 2022, 55, 5342−5352 Read Online

ACCESS | Metrics & More | Article Recommendations | Supporting Information

ABSTRACT: The oligomers in polymer materials have a decisive influence on properties. However, there is a lack of studies on the oligomers in polycaprolactone (PCL), and the effect of oligomers on material performance has not yet been revealed. In this work, the oligomer content in PCL was quantitatively characterized, and the result refers that the cyclic dimer content reaches 97 wt % in the PCL oligomer. In addition, the effect of oligomers on the thermal behavior, the *in vitro* degradability, and the *in vitro* cytotoxicity cell experiments were further investigated. In the *in vitro* degradation simulation experiments, the PCL with a higher content of oligomers showed faster degradation than that with a lower content of oligomers. Moreover, the *in vitro* cytotoxicity cell experiments proved that increasing the content of oligomers can greatly improve the biocompatibility of PCL materials. These results can help researchers better understand oligomers and promote the application of PCL more directly.

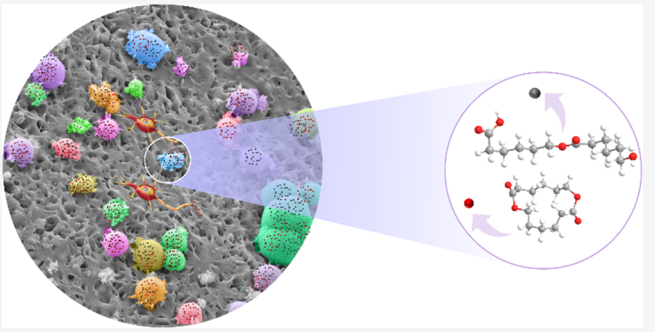

1. INTRODUCTION

Ring-opening polymerization (ROP) and polycondensation reactions are adopted to synthesize polymers in a vast majority of cases. A certain amount of "linear" and "cyclic" byproducts, namely, oligomers, is ineluctably produced in these processes.[1] On the one hand, the generated cyclic oligomers increase the difficulties in preparation and downstream processing and even pose a potential risk to the human body when equipped with clothes, films, or medical devices.[2,3] Literature and industrial cases on polyamide 6 (PA6) and polyester (PET) have disclosed that the oligomers tended to block the vacuum tube and spinneret during the production process. More worryingly, on the other hand, the oligomer content influences the application performance of polymer materials.[4,5] A decrease of the oligomer content in PA6 can increase the melting temperature of polymers.[1,6,7] In addition, the low content of oligomers in PET, polybutylene terephthalate (PBT), and polypropylene (PP) reduced the potential risks to the human environment triggered by the migration of oligomers.[3,8−10] However, some studies revealed that adding a certain amount of chitosan oligomers can increase the anti-cancer effect of a material.[11] Therefore, understanding the physical and chemical properties of oligomers and their effects on materials is extremely important for scientific regulation of the oligomer content in polymers and thus green and safety application of these materials.

The conversion rate and residue content of oligomers vary greatly in different polymers, and the influence of oligomers on the properties of materials is highly dependent on the detailed situation. PCL, as a biodegradable material, has increasingly attracted many researchers' attention due to its wide application in biomedical equipment, degradable films, sealing devices, and environmentally friendly coatings.[12−16] A definite knowledge of oligomers in PCL is the presence of cyclic oligomers.[17] With effort, our recent studies revealed the "backbiting" mechanism of oligomer formation in PCL, and a catalytic strategy was established for oligomer regulation in this polymer.[18] However, how to separate and purify the oligomers from PCL, especially determine the influence of oligomer content in PCL on material properties, still needs to be expounded.

In this work, to quantificationally unveil the mystery masks of oligomers in PCL, we first established a simple operation for separating and purifying PCL oligomers. In addition, the chemical and physical properties of cyclic dimers were systematically described. Furthermore, the oligomer content's influence on the mechanical properties, thermal stability, biodegradability, and *in vitro* cytotoxicity of PCL was uncovered. These findings disclosed that the samples with more oligomers showed greater surface defects in the later stages of degradation and induced more hydroxyapatite to deposit in simulated body fluids. Especially, the *in vitro*

Received: February 7, 2022
Revised: June 16, 2022
Published: June 30, 2022

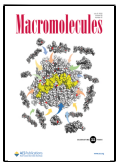

https://doi.org/10.1021/acs.macromol.2c00275
Macromolecules 2022, 55, 5342−5352

cytotoxicity test showed that the samples with a higher oligomer content had better biocompatibility. These results can help researchers better understand oligomers and promote the application of PCL more directly.

2. EXPERIMENTATION

2.1. Raw Materials and Reagents. ε-Caprolactone (CL) was obtained from Hunan Juren Chemical Technology Co., Ltd. Acetonitrile (chromatographically pure) and deuterated chloroform were purchased from Shanghai Aladdin Biochemical Technology Co., Ltd. Chromatographically pure toluene, methanol, and chloroform were bought from Sinopharm Chemical Reagent Co., Ltd. Mouse mesenchymal stem cells, DMEM/F-12 medium, and fetal bovine serum were all from Thermo Fisher, and calcein-AM/PI stains were provided by Beijing Biolab Technology Co., Ltd. The simulated body fluid used for the contact angle test was purchased from Dongguan Chuangfeng Automation Technology Co., Ltd., and the preparation methods of PCL with different oligomer contents in this study are presented in Tables S1 and S2 of the Supporting Information.

2.2. Single-Crystal Culture. The mixed oligomers were collected according to the method in the Supporting Information, and the resulting mixed oligomers were dried in a vacuum oven at 25 °C for 12 h and then washed with ethanol to remove surface impurities and dried by vacuum again. Preliminarily purified mixed oligomers (0.5 g) were dissolved in toluene to make a 0.1 g/mL solution, and a small reagent bottle containing 2 mL of the above solution and a large reagent bottle containing deionized water were stacked and sealed.

Using a capillary tube, the abovementioned samples were taken every 1 h and placed under a polarizing microscope for observation. When the size of most of the crystals is between 0.2 and 0.5 mm and the special color of the crystal appears, the sample can be tested by X-ray single-crystal diffraction. Excess crystal samples are reserved for subsequent testing.

2.3. Characterization. The above crystal samples were completely dissolved in deuterated chloroform. The spectrum of the product was recorded with BRUKER AVANCE-500 series ^{1}H NMR and ^{13}C NMR spectrometers.

X-Ray data were taken on an Agilent Supernova X-Ray diffractometer equipped with a large area CCD detector.

The thermal properties of the single crystal were tested with a NETZSCH DSC200F3 differential scanning calorimeter (DSC, Germany). In brief, a 5 mg sample was taken and the thermal history was eliminated through a gradual increase of the temperature from 30 to 200 °C. After the temperature was kept constant for 3 min, the temperature was lowered to −100 °C, and then the temperature was kept constant for another 3 min. The process was continued until the temperature increased to 200 °C.

A NETZSCH STA-4O9PC comprehensive thermal analyzer (Germany) was used to test the thermal stability of the sample. The test temperature ranged from 30 to 800 °C, and the heating rate was 10 °C/min.

The enriched single-crystal particle was selected to observe the morphology change of the target object by adjusting the intensity of the polarized light and the temperature of the hot stage. The polarizing microscope (POM) model was from Shanghai Changfang Optical Instrument Co., Ltd., N-type.

Dynamic contact angle tests were performed using LAUDA Scientific GmbH, LSA-100 models with the as-prepared PCL containing 4.3 and 12.5 wt % oligomer and commercial PCL (oligomer content of 8.3 wt %). Test time was 20 min. The test solvent was simulated body fluid. The test results were angled using ImageJ software.

Bruker Multimode 8 atomic force microscopy (AFM) was used to characterize the surface morphology of the sample; all measurements were performed in the semi-contact mode using a 0.01−0.025 ohm·cm antimony(n)-doped Si probe NSG10 tip with a resonance frequency of 140−390 kHz, a force constant of 3.1−37.6 N/m, and an image of 2 × 2 μm^2.

X-ray photoelectron spectroscopy (XPS) of the samples with an oligomer content of 4.3 and 12.5 wt % was done using a Thermo Fisher Scientific 250Xi. The base pressure in the testing chamber was approximately 6 × 10^{-8} Pa. The test elements were C and O. During the test, the specimens were etched five times, and the spectra were acquired, each with an etching depth of 20 nm. The samples were excited by X-rays in a 400 μm spot area with a monochromatic Al K$\alpha_{1,2}$ radiation of 1486.6 eV, and the test spectra were fitted using Thermo Avantage software provided with the instrument.

2.4. Establishment of the Oligomer Liquid Phase Standard Curve. Pure acetonitrile was used as a blank sample, and the obtained single crystal was dissolved in acetonitrile to make a 0.1 g/L solution. Its maximum UV absorption wavelength in the acetonitrile solution was tested. At the same time, the test method for the maximum absorption wavelength of the mixed oligomer and the caprolactone in acetonitrile was the same as that of the single crystal. The test instrument model was a Canadian PTI QM40 with a signal-to-noise ratio of 10,000:1 and wavelength accuracy of 0.06 nm.

We took 1, 2, 3, 4, 5, 6, 7, 8, and 9 mL of the above-prepared single-crystal solution in sequence and placed them in a volumetric flask with acetonitrile by a gradient dilution method; the total solution volume was 10 mL. The configuration method of the caprolactone and the mixed oligomer was the same as that above. The test conditions were the following: detector: UVIS-201 UV detector; chromatographic column: Altima C18 column 4.6 mm × 250 mm × 5 μm; mobile phase: acetonitrile/water mixed mobile phase gradient elution; column temperature: 30 °C, flow rate: 1.0 mL/min; and wavelength: 220 nm.

2.5. *In Vitro* Degradation of Samples. Samples for the degradation test were weighed, classified, and labeled before the test. The degradation cycles were of 0 (0 W), 2 (2 W), 4 (4 W), 6 (6 W), 8 (8 W), 12 (12 W), 16 (16 W), 20 (20 W), and 24 weeks (24 W). The test temperature was kept at 37 °C, and the oscillation frequency was 10 Hz. When the degradation was over, the masses of the samples were weighed again after vacuum drying so that the weight loss rate could be calculated.

A Changchun Kexin electronic universal testing machine was used to test the tensile strength of the splines before and after degradation. Before the test, the specimens were vacuum-dried and cut into dumbbell-shaped specimens of 0.5 × 4 × 60 mm^3 with a punching machine, and the tensile strength was measured at a speed of 5 mm/min. Each sample was tested five times, and the average value was recorded.

The surface morphologies of the degraded sample were observed using the scanning electron microscope. Before the test, gold was sprayed with a VGC-1200 ion sputtering instrument from Zhongke Instrument Co., Ltd. The scanning electron microscope model was MIRA3LMH from TESCAN, Czech Republic, and the EDS model was XMAX20 from Oxford, England.

https://doi.org/10.1021/acs.macromol.2c00275
Macromolecules 2022, 55, 5342−5352

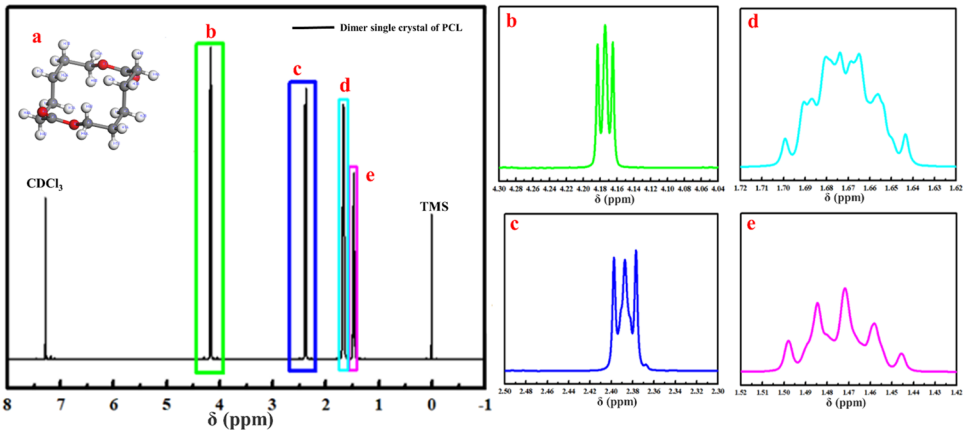

Figure 1. Single-crystal structure of the cyclic dimer (a); ^{1}H NMR spectrum of the single crystal (b–e).

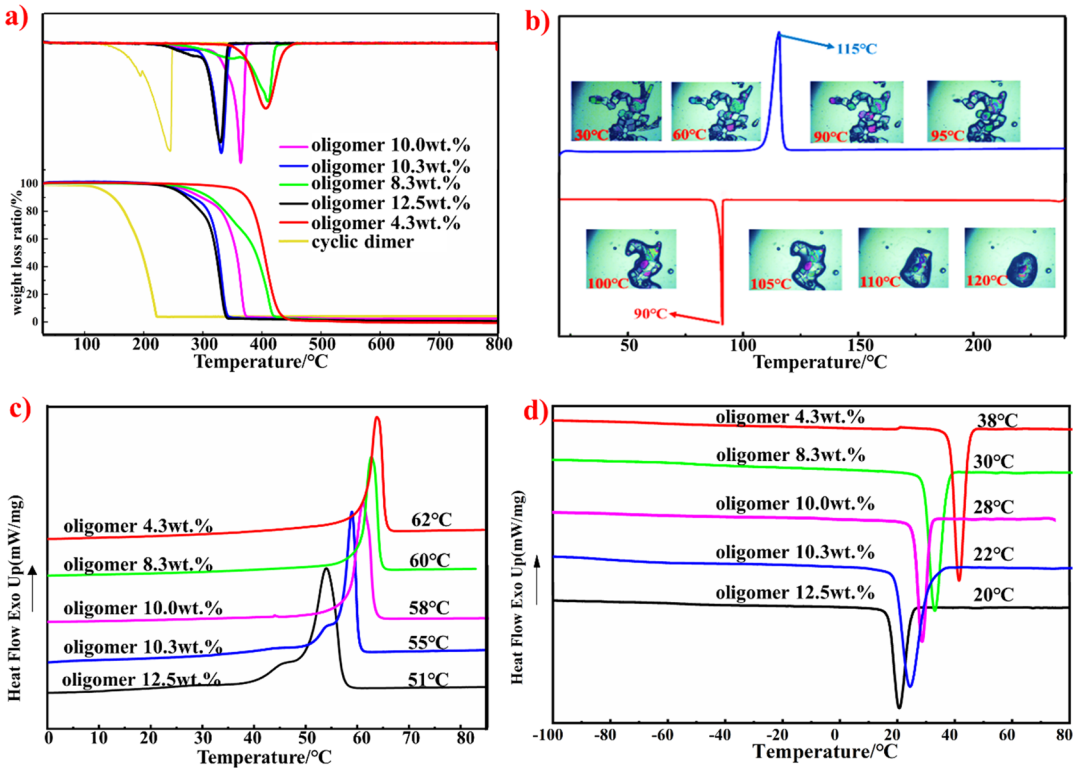

Figure 2. (a) TG thermogram of the CL_2 single crystal and PCL with different oligomer contents; (b) DSC and POM test results of the single crystal; and (c, d) DSC thermogram test results of PCL with different oligomer contents.

2.6. *In Vitro* Cytotoxicity Test of Samples. The processed PCL samples were placed in a 12-well plate and soaked in the DMEM/F-12 culture medium for 24 h to remove the residual toxicity of the material. Each well was inoculated with 2×10^4 CFU/mL cells according to the MTT method (cell lines: mouse mesenchymal stem cells; see raw materials in Section 2.1).[19] The above plate was cultured at 37 °C temperature, 5% CO_2, and 90% relative humidity. Meanwhile, each group of samples was set with at least five groups of control samples. The culture times were 1, 2, and 3 days. Each culture stage needed an appropriate amount of MTT and DMSO to be added, which was transferred to the 96-well plate in time. We used an American Synergy HTX BIOTEK type microplate reader to detect the optical density value (OD) value, and the test wavelength was 492 nm.

The samples were taken out in time after incubation for 1, 2, and 3 days, then rinsed with PBS buffer solution, and stained with 1 mL of DMEM/F-12 and calcein-AM/PI live/dead solution for 15 min. After that, a Leica SP8 fluorescence microscope (Germany) was used to detect cell proliferation at a wavelength of 488 nm.

3. RESULTS AND DISCUSSION

3.1. Structural Analysis. The cyclic dimer was the dominant component of oligomers[6] and showed a great negative influence on the properties of materials. The structure of the obtained single crystal in this work was analyzed and is shown in Figure 1a. Figure 1b shows a peak at 4.20–4.14 ppm, which is the characteristic hydrogen chemical shift of the methylene group connected to the ester bond (O═C–O–CH_2),[20] The "c" position is the characteristic hydrogen

https://doi.org/10.1021/acs.macromol.2c00275
Macromolecules 2022, 55, 5342–5352

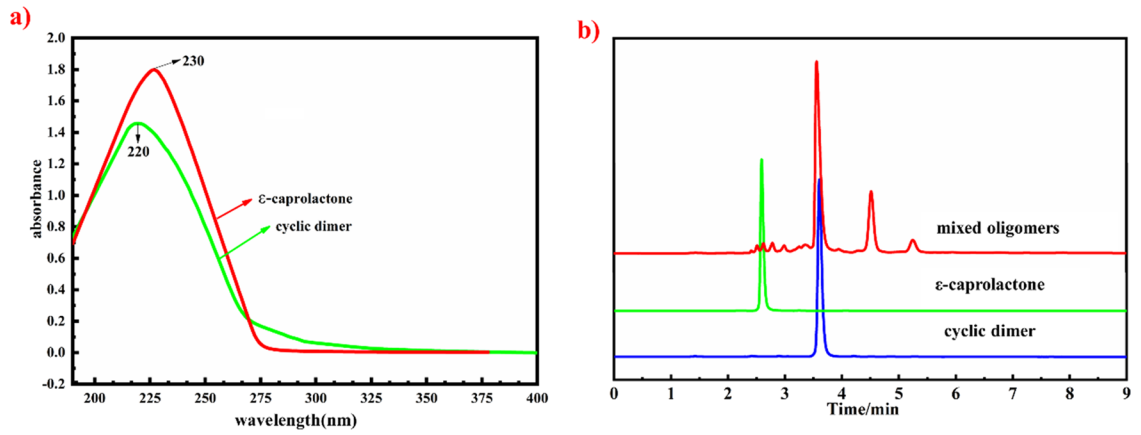

Figure 3. (a) UV−vis spectra. (b) HPLC chromatogram.

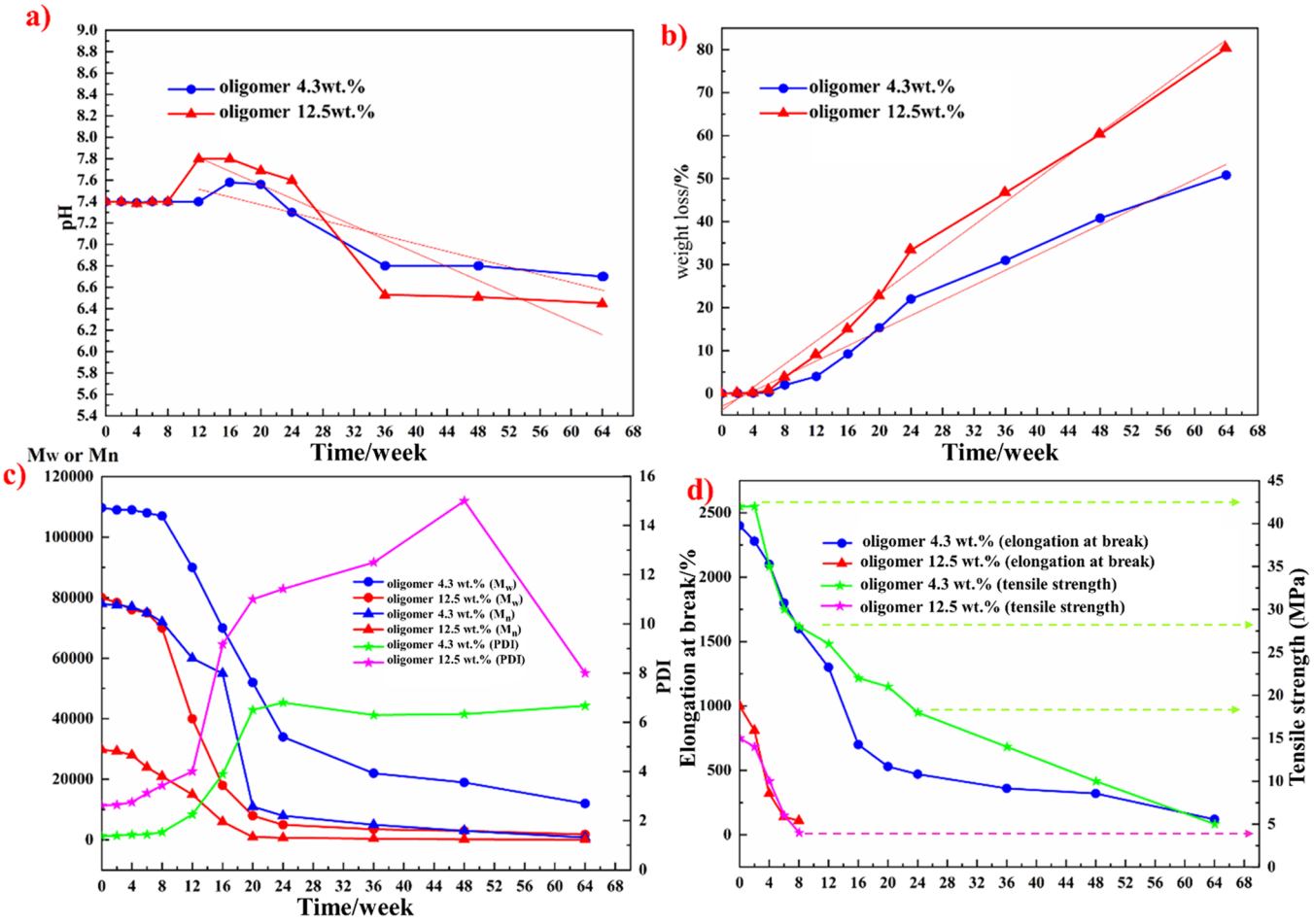

Figure 4. (a) PCL with different oligomer contents simulated the change of the pH value of body fluid during degradation; (b) weight change of PCL with different oligomer contents during degradation; (c) change of Mn\Mn\PDI of PCL with different oligomer contents during degradation; (d) changes of mechanical properties of PCL with different oligomer contents during degradation.

chemical shift of the methylene group directly connected by the (O═C−CH_2) carbonyl bond.[21] "d" and "e" are assigned as the characteristic chemical shifts of the methylene group (−CH_2).[22] Among them, there is a fivefold peak at "e" and a 10-fold peak at "d". In addition, the structure of the obtained PCL cyclic dimer was re-verified by ^{13}C NMR (Figure S1). This indicates that the substance may be a 14-membered ring lactone compound.

A further X-ray single-crystal diffraction test was performed on the crystals obtained from the mixed oligomers. The test conditions and the basic structural parameters of the crystal are shown in Table S3. According to the test results, the structural formula of the compound is confirmed to be $C_{12}H_{20}O_4$ and has a molecular weight of 228.28. The spatial structure of the *x*, *y*, and *z* axes is shown in Figure S3. These results proved that the obtained oligomers are cyclic dimers.

https://doi.org/10.1021/acs.macromol.2c00275
Macromolecules 2022, 55, 5342−5352

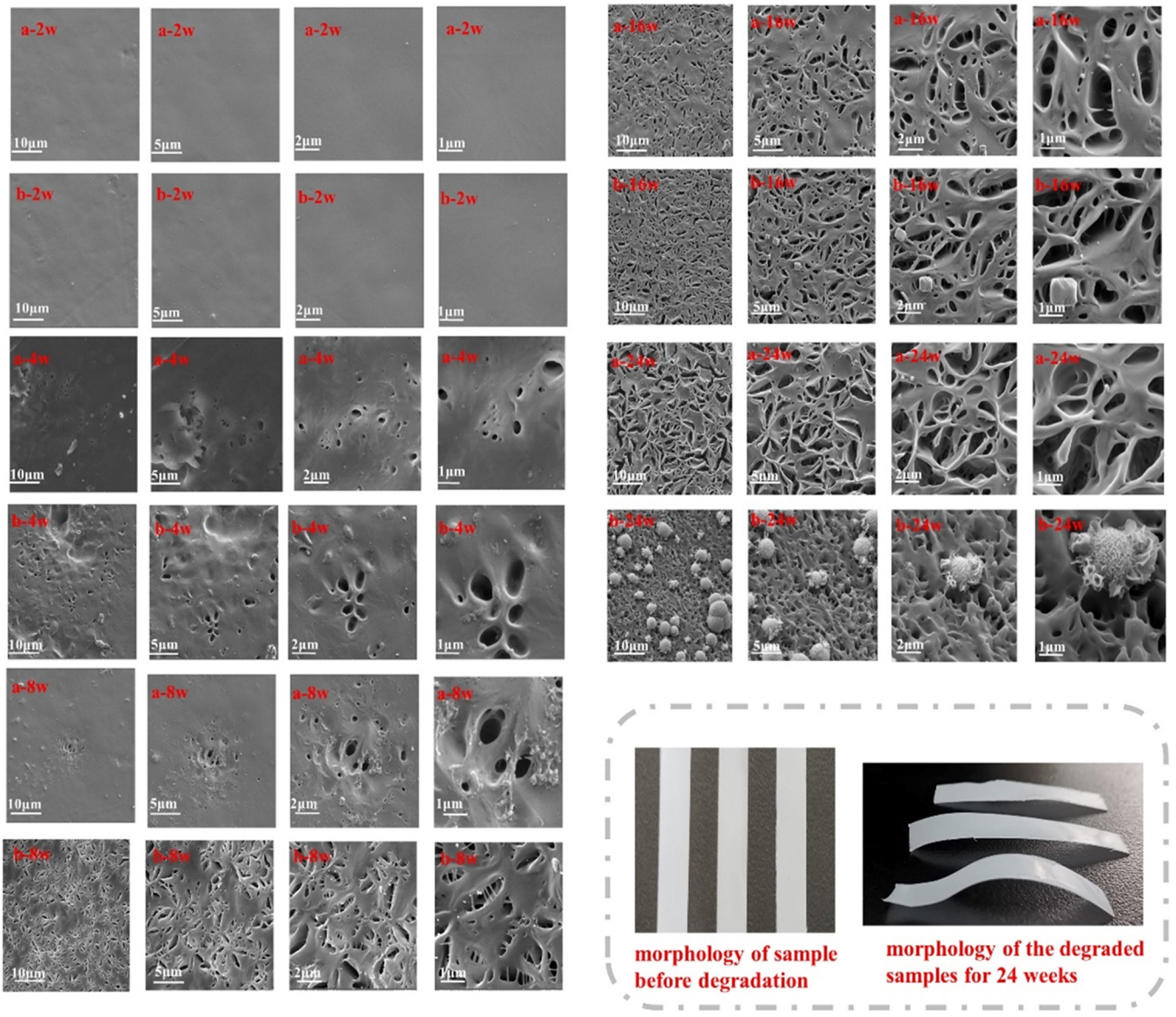

Figure 5. SEM images of different degradation cycles of PCL with different oligomer contents and samples with 12.5 wt % oligomer content. The physical morphology of the spline after 24 weeks of degradation: (a) oligomer content is 4.3 wt % and (b) oligomer content is 12.5 wt %.

3.2. Polarizing Microscope (POM) and Thermal Stability Analysis. The thermal stability of the cyclic dimer single crystal was investigated under a POM. As shown in Figure 2b, it is interesting to observe only liquid in the shape of a droplet remaining in the field of view when the temperature rises to 120 °C. This indicates that the melting temperature of this single crystal is approximately 120 °C, which is close to the DSC test result (Figure 2b). Further analysis (Figure 3a) shows that the complete decomposition temperature ($T_{d100\%}$) of CL_2 is 237.14 °C (Table S4). In addition, the melting temperature and crystallization temperature of PCL were deeply influenced by its oligomer content. PCL with an oligomer content of 4.3 wt % showed a melting temperature of 62 °C and a crystallization temperature of 38 °C (Figure 2c,d). With the content of oligomers rising to 12.5 wt %, the melting temperature and the crystallization temperature of PCL significantly decreased to 51 and 20 °C, respectively (Figure 2c,d). According to published reports, it may be that the oligomers act as a lubricant for the molecular chain, therefore lowering the melting temperature of the material.[6,23,24]

Moreover, it is obvious that, from Figure 2a, as the content of oligomers increases, the thermal decomposition temperature shows a downward trend. The PCL sample with the lowest oligomer content presents a complete decomposition temperature of 446 °C, which is 96 °C higher than the sample with the highest oligomer content. Table S4 details the TG data of the CL_2 crystal and PCL. Based on this, we believe that the existence of CL_2 in the target product would harm the thermal stability of the material.

3.3. Establishment of the Standard Curve of CL_2 and CL in PCL. The standard curves of caprolactone and CL_2 were further fitted to calculate the content of oligomers in PCL. During the course, the maximum ultraviolet absorption wavelength of CL_2 and CL acetonitrile solutions was tested, and 220 nm was selected as the test absorption wavelength (Figure 3a). An acetonitrile:water 10:1 gradient elution was used for the test. Based on Figure 3 and the liquid phase

https://doi.org/10.1021/acs.macromol.2c00275
Macromolecules 2022, 55, 5342−5352

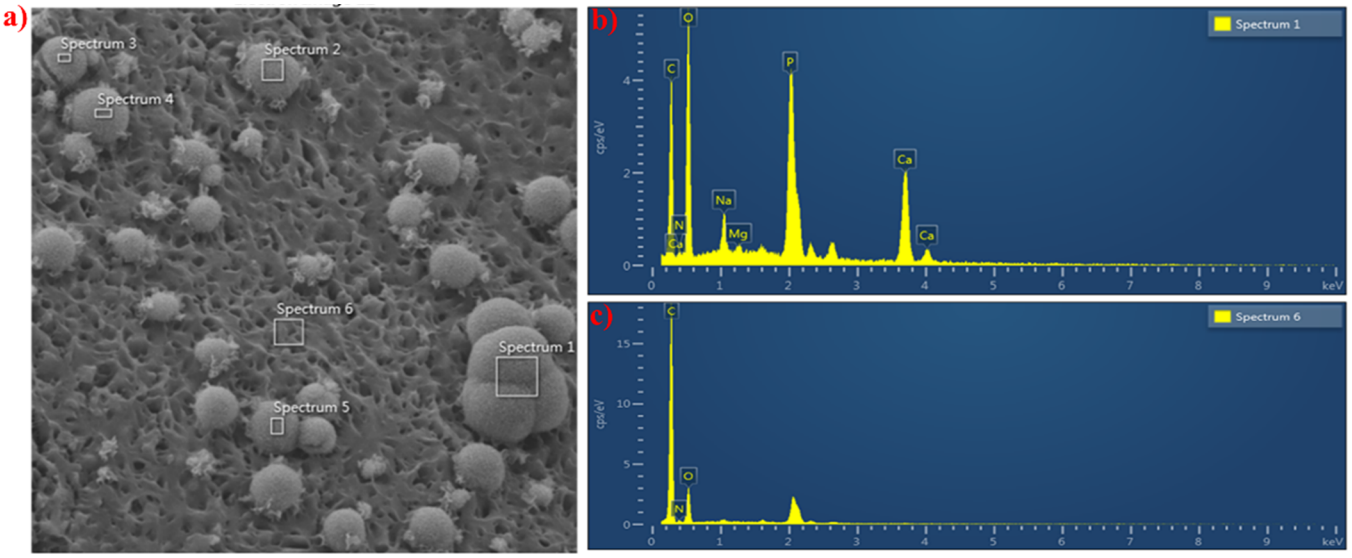

Figure 6. (a) SEM images of PCL samples containing 12.5 wt % oligomers after 24 weeks of degradation; (b, c) EDS spectra of spectra 1 and 6 in panel a.

integral data, the CL_2 content in the mixed oligomer is calculated to be as high as 97 wt %, while the other components only account for 3 wt % (Figure 3b and Figure S2). It can be preliminarily learned that the main component in the mixed oligomer is CL_2. In other words, among all oligomers, the cyclic dimer is of great importance to the overall performance of PCL. We deeply believe that this discovery could inspire researchers on how to prepare PCL with high performance through reasonably regulating the oligomers in the polymer.

3.4. Degradation Analysis. PCL with 4.3 and 12.5 wt % oligomer content was selected and placed in a biological constant-temperature shaking box to conduct a simulated body fluid (SBF) *in vitro* degradation control test for up to 64 weeks. In the first 8 weeks, it can be seen from Figure 4a that the mass of the two groups of samples and the pH value, together with the mass of the soaking solution, did not change much. However, when the degradation cycle was prolonged, the degradation soaking solution gradually became weakly acidic, inferring that lots of degraded artifacts were released. The results also proved that the weight loss rate of the samples with a high oligomer content was even greater. After 64 weeks, the weight loss of PCL with 12.5 wt % oligomer content was as high as 80% (Figure 4b).

The change in relative molecular weight is even more significant. Even if the degradation cycle of the sample with an oligomer content of 4.3 wt % is as long as 64 weeks, its relative molecular weight remains 12,000 (Figure 4c). There is a big gap compared to the reported result that human cells can absorb polymer fragments with a molecular weight of 5000 and below.[25] In this case, the low content of oligomers in PCL played a negative role in PCL degradation, thus making it much more difficult to be absorbed by cells in a short time.

In addition, as shown in Figure 4d, the mechanical properties of the sample with an oligomer content of 12.5 wt % can no longer be evaluated after 8 weeks of degradation. However, the sample with an oligomer content of 4.3 wt % remains to have an elongation at a break of 120% and a tensile strength of 5 MPa when the degradation cycle lasted 64 weeks. This shows that, although the mechanical strength of the material has been damaged to a certain extent during the long-term degradation process, it still maintained the characteristics of a tough material. In addition, unlike the results of the weight loss rate, pH, and relative molecular weight, the mechanical properties of samples showed a sharp decline in the first 8 weeks. This phenomenon indicates that the material has undergone major changes in the microstructure during the degradation and soaking process and its broken or short-term "swelling" molecular segments acted as "stress concentration points" or "cracks" when subjected to external forces.[26−28] Based on this, it can be concluded that the degradation of the samples with a higher oligomer content is more in line with the biodegradation requirements of human implant materials because they have greater internal "defects" during the degradation process.[28−30]

Furthermore, the degradation samples were vacuum-dried and then analyzed by scanning electron microscopy. It can be seen from Figure 5 that all samples appear with a smooth surface morphology after 2 weeks of degradation. However, from the 4 week data, holes were observed to appear on the surface. Compared to the sample with 4.3 wt % oligomers, larger "holes" on the surface of samples containing 12.5 wt % oligomers were observed. More interesting, the holes appearing on the surface of the material became denser during the whole degradation period. When the degradation period was extended to 24 weeks, the sample surface was fully occupied by "holes". According to the literature, this kind of densely distributed "hole" in the form of a network can effectively increase the specific surface area of material, making it better than ordinary materials when used as a drug-loaded sustained release.[31,32]

Amazingly, as the degradation time increased, some spherical particles were deposited on the surface of the degraded samples with higher oligomer contents (Figure 6a and Figure S6). Further EDS analysis was performed to reveal the detail component of spherical particles as shown in spectrum 1 (Figure 6b) and spectrum 6 (Figure 6c). By comparing the base elements based on the EDS energy spectrum, it is found that the spherical particles mainly contain Ca and P elements. The Mg and N elements are most likely

https://doi.org/10.1021/acs.macromol.2c00275
Macromolecules 2022, 55, 5342−5352

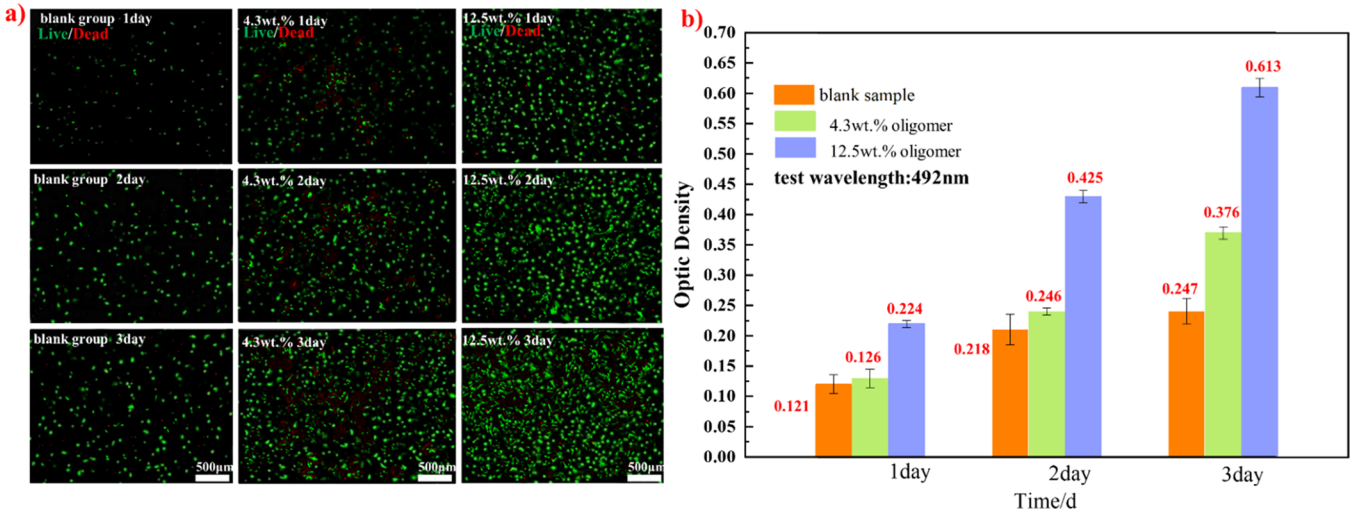

Figure 7. (a) Fluorescence staining photos of live/dead cells of PCL surface cell cultures with different oligomer contents; (b) MTT test results of PCL surface cell culture with different oligomer contents.

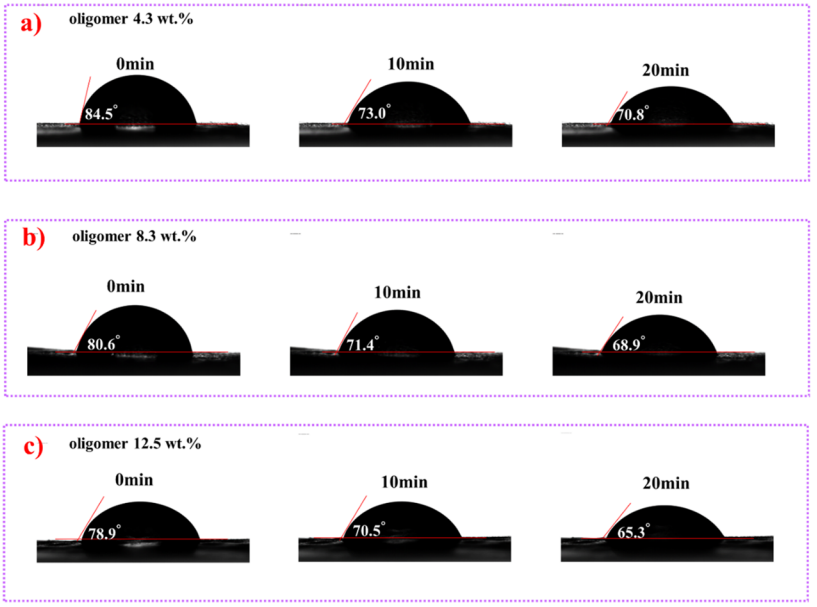

Figure 8. (a–c) Simulated body fluid dynamic contact angle tests with oligomer contents of 4.3, 8.3 (commercial products), and 12.5 wt % in PCL.

coming from the components in the simulated body fluid (SBF), so the deposited particles on the surface of the sample may be hydroxyapatite (HA).[33,34] According to reports, the presence of HA will greatly improve the compatibility of the material implanted into the organism.[35,36] Combining the analysis of the degradation SEM image with the EDS energy spectrum, it can be seen that the sample with an oligomer content of 12.5 wt % has better biocompatibility with the extension of the degradation cycle and releases more oligomers in the same cycle. The degradation rate of the sample is significantly faster than that of the sample with less oligomer content.

3.5. Cytotoxicity Results. Cell proliferation was obtained by the MTT method.[37] Figure 7 shows the proliferation of MTT cells when BMSC was cultured on the surface of PCL samples with different oligomer contents for 1, 2, and 3 days. The results showed that the OD value gradually increased as the culture time increased (Figure 7b). The sample containing more oligomers showed better proliferation tendency than the sample with less oligomer content. This indicates that the increase in the oligomer content is conducive to cell proliferation to a certain extent, which refers that the material exhibits better cell compatibility.

It can be seen from the calcein-AM/PI live and dead cell fluorescence staining chart that the oligomers effectively promoted the growth of cells in the PCL sample. During the same incubation time, the number of viable cells in the two groups of samples is much more than that in the blank sample, and the sample containing a lower oligomer content has a much greater viable cell density. In the later period of culture, living cells tended to aggregate into multilayered cells. During the same incubation time, the density of dead cells in the sample with 12.5 wt % oligomers was higher than that of the blank sample. It infers that its cytocompatibility is lower than the sample with 4.3 wt % oligomers. These results fully indicate that increasing the oligomer content is beneficial to promoting the cell compatibility of PCL materials.

https://doi.org/10.1021/acs.macromol.2c00275
Macromolecules 2022, 55, 5342−5352

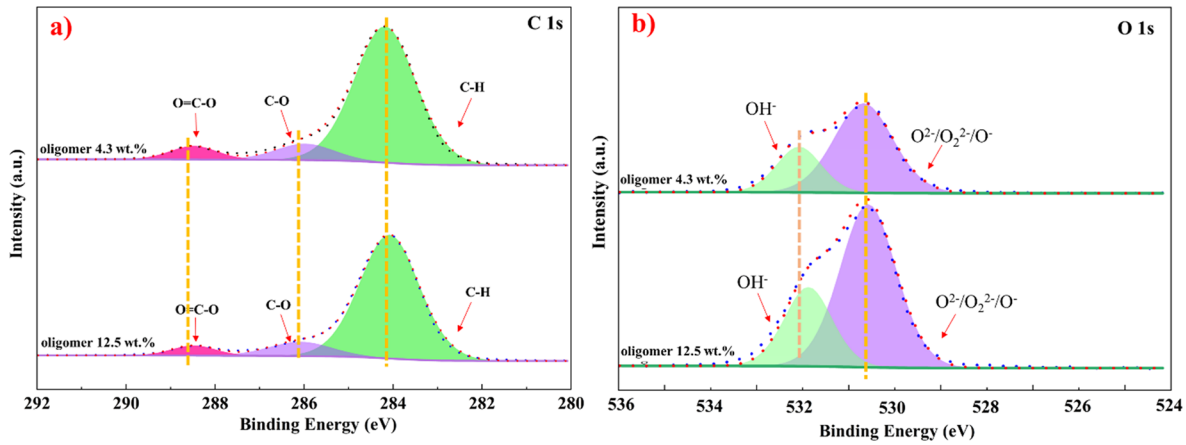

Figure 9. (a, b) C 1s spectrum and O 1s spectrum of the XPS test for samples with oligomer contents of 4.3 and 12.5 wt %.

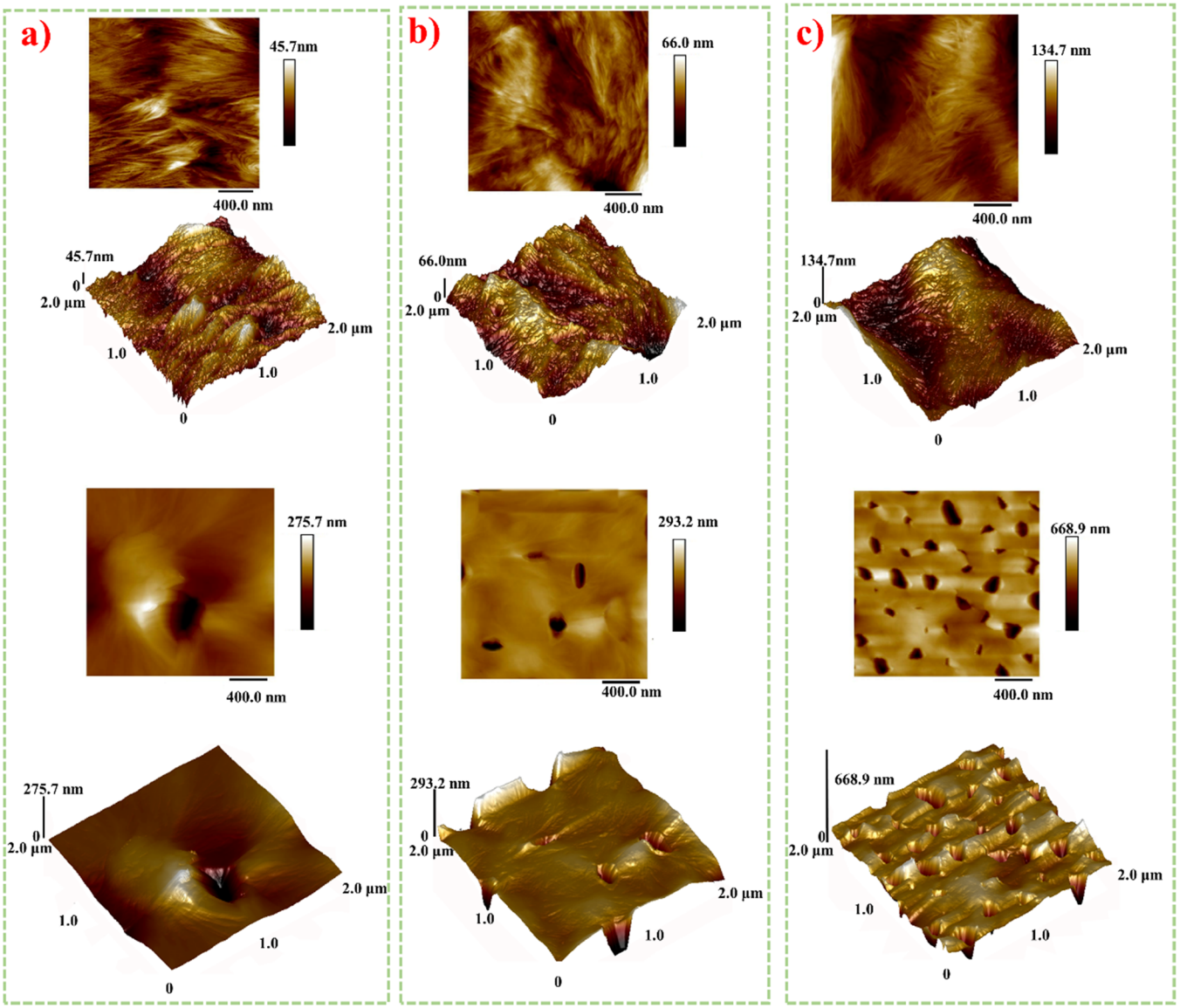

Figure 10. (a–c) AFM test for samples with oligomer contents of 4.3, 8.3, and 12.5 wt % before degradation and degradation of 24 W samples.

3.6. Mechanism of Cell Adsorption. The adsorption mechanism of polymer materials to cells or proteins has always been a difficult research point for bio-based materials.[38,39] After years of development, there have been many ways to make preliminary elaborations on the mechanism of this aspect. In this case, we performed simulated humoral dynamic

https://doi.org/10.1021/acs.macromol.2c00275
Macromolecules 2022, 55, 5342−5352

contact angle, XPS, and AFM tests on the samples with an oligomer content of 4.3 and 12.5 wt % and commercial PCL.[38−40] From Figure 8, it can be seen that the initial contact angle of the sample with an oligomer content of 12.5 wt % is 5.6° lower than that of the sample with a polymer content of 4.3 wt %. After a dynamic test for 20 min, the sample with a higher oligomer content still keeps a smaller contact angle. According to literature reports, materials with smaller contact angles are more hydrophilic.[39] The results infer that the PCL sample containing more oligomers is more hydrolytic.

Further XPS tests were conducted to confirm whether there are more hydrophilic groups in the specimen with more oligomer content (Figure 9). It is found that the oligomer content has no practical effect on the carbon content in the C 1s spectra. However, the O 1s spectra show that there are two strong signal peaks for the sample with 12.5 wt % oligomers. One is attributed to OH^- groups, and the other is assigned to oxygen-binding groups. Additionally, the intensity is significantly higher than that of the sample containing 4.3 wt % oligomers. The same phenomenon was observed in different etching depths (Figures S7 and S8), which infers that the oligomer has changed the surface properties of the material and could help the material to promote cell adsorption performance.[41]

To better illustrate this phenomenon, the surface morphologies of the samples with an oligomer content of 4.3 and 12.5 wt % and the commercial PCL specimens before and after degradation were analyzed by AFM (Figure 10). The test results show that the surface of samples with an oligomer content of 12.5 wt % is rougher than that of samples with a lower oligomer content. The former SEM results have proved that the samples with a high oligomer content could deposit hydroxyapatite in simulated body fluid at the later stage of degradation. Thereby, it can be inferred that the rough surface of the sample with a high oligomer content can be conducive to the deposition of bioactive substances, such as hydroxyapatite in simulated body fluid, to improve the biocompatibility of the material.

4. CONCLUSIONS

The caprolactone cyclic dimer was successfully separated from PCL oligomers, and the single crystal was cultured. The content of the cyclic dimer reached 97 wt % PCL oligomers. The thermal decomposition temperature of the cyclic dimer is 210 °C and lower than that of PCL. It was found that oligomers could significantly damage the thermal stability and the mechanical properties of PCL. However, the degradation effect of the sample with an oligomer content of 12.5 wt % was significantly better than that of the sample with an oligomer content of 4.3 wt %, enabling a certain amount of hydroxyapatite to be deposited in the late stage of degradation. Moreover, the oligomers greatly affected the roughness of the sample's surface and the number of hydrolytic groups, thus significantly promoting the adsorption and growth of cells in the PCL sample. It is believed that these results can help researchers better understand oligomers in PCL so that we can promote the application of PCL in more direct scenarios. In the future, we will further learn the effect of oligomers on the degradability of PCL materials and cell compatibility in detail.

■ ASSOCIATED CONTENT

Supporting Information

The Supporting Information is available free of charge at https://pubs.acs.org/doi/10.1021/acs.macromol.2c00275.

Process parameters for PCL preparation, low-field ^{1}H NMR test results of synthesized samples containing PCL with different oligomer contents, basic parameters of cyclic dimer single crystals in mixed oligomers, specific data of TG test between CL_2 and PCL, ^{13}C NMR spectra of cyclic dimer, standard curve spectra of CL and CL_2, schematic diagram of the single-crystal *xyz* structure, proposed mechanism for catalyst initiation process, "coordination−insertion" mechanism for the propagation, possible "backbiting" reactions of the tetraphenyl tin catalytic system, SEM images of PCL samples containing 12.5 wt % oligomers after 24 weeks of degradation, XPS survey of different etching depths for samples with oligomer contents of 4.3 and 12.5 wt %, and C and O elements with different etching depths of samples with oligomer contents of 4.3 and 12.5 wt % (PDF)

■ AUTHOR INFORMATION

Corresponding Authors

Xi Wang − *National & Local Joint Engineering Laboratory for New Petro-chemical Materials and Fine Utilization of Resources, Hunan Normal University, Changsha 410081 Hunan, P. R. China*; Phone: +86-137877782496; Email: wangxiiccas@hotmail.com

Chunwang Yi − *National & Local Joint Engineering Laboratory for New Petro-chemical Materials and Fine Utilization of Resources, Hunan Normal University, Changsha 410081 Hunan, P. R. China*; orcid.org/0000-0003-4398-8058; Phone: +86-13787224901; Email: cwyi@hunnu.edu.cn

Authors

Caihong Gong − *National & Local Joint Engineering Laboratory for New Petro-chemical Materials and Fine Utilization of Resources, Hunan Normal University, Changsha 410081 Hunan, P. R. China; School of Materials Science and Engineering, South China University of Technology, Guangzhou 510641, P. R. China*

Yu Gu − *National & Local Joint Engineering Laboratory for New Petro-chemical Materials and Fine Utilization of Resources, Hunan Normal University, Changsha 410081 Hunan, P. R. China*

Complete contact information is available at: https://pubs.acs.org/10.1021/acs.macromol.2c00275

Notes

The authors declare no competing financial interest.

■ ACKNOWLEDGMENTS

This research was supported by the enterprise funds from Hunan Juren Chemical New Mstar Technology, Co., Ltd.: National Key Research Program of China (grant no. 2016YFB0302702); and Open Foundation of National & Local Joint Engineering Laboratory for New Petro-chemical Materials and Fine Utilization of Resources (grant no. KF201804). C.G. also sincerely thanks Dr. Ronghui Liu for his help in the writing of this article.

REFERENCES

(1) Peng, S.; Peng, L.; Yi, C.; Zhang, W.; Wang, X. A novel synthetic strategy for preparing semi-aromatic components modified polyamide 6 polymer. *J. Polym. Sci., Part A: Polym. Chem.* **2018**, *56*, 959−967.

(2) Hoppe, M.; de Voogt, P.; Franz, R. Oligomers in polyethylene naphthalate and polybutylene terephthalate − Identification and exploring migration. *Food Packag. Shelf Life* **2018**, *17*, 171−178.

(3) Ragusa, A.; Svelato, A.; Santacroce, C.; Catalano, P.; Notarstefano, V.; Carnevali, O.; Papa, F.; Rongioletti, M. C. A.; Baiocco, F.; Draghi, S.; D'Amore, E.; Rinaldo, D.; Matta, M.; Giorgini, E. Plasticenta: First evidence of microplastics in human placenta. *Environ. Int.* **2021**, *146*, No. 106274.

(4) Paseiro-Cerrato, R.; Noonan, G. O.; Begley, T. H. Evaluation of Long-Term Migration Testing from Can Coatings into Food Simulants: Polyester Coatings. *J. Agric. Food Chem.* **2016**, *64*, 2377−2385.

(5) Canellas, E.; Vera, P.; Song, X.-C.; Nerin, C.; Goshawk, J.; Dreolin, N. The use of ion mobility time-of-flight mass spectrometry to assess the migration of polyamide 6 and polyamide 66 oligomers from kitchenware utensils to food. *Food Chem.* **2021**, *350*, No. 129260.

(6) Yi, C.; Yang, C.; Li, J.; Chen, J.; Zhang, S.; Sun, H. Agglomeration behaviour of caprolactam solution concentrates triggered by cyclic dimers in the recovery process: Characterisation, mechanism, and process optimisation. *Process Saf. Environ. Prot.* **2020**, *136*, 56−65.

(7) Klun, U.; Andrenšek, S.; Kržan, A. Electrospray mass spectrometry determination of linear and cyclic oligomers of polyamide-6. *Polymer* **2001**, *42*, 7095−7099.

(8) Brenz, F.; Linke, S.; Simat, T. J. Linear and cyclic oligomers in PET, glycol-modified PET and Tritan™ used for food contact materials. *Food Addit. Contam., Part A* **2021**, *38*, 160−179.

(9) Eckardt, M.; Schneider, J.; Simat, T. J. In vitro intestinal digestibility of cyclic aromatic polyester oligomers from polyethylene terephthalate (PET) and polybutylene terephthalate (PBT). *Food Addit. Contam., Part A* **2019**, *36*, 1882−1894.

(10) Brenz, F.; Linke, S.; Simat, T. Linear and cyclic oligomers in polybutylene terephthalate for food contact materials. *Food Addit. Contam., Part A* **2018**, *35*, 583−598.

(11) Daraghmeh, N. H.; Chowdhry, B. Z.; Leharne, S. A.; Al Omari, M. M.; Badwan, A. A. Chapter 2 − Chitin. In *Profiles of Drug Substances, Excipients and Related Methodology*; Brittain, H. G., Ed. Academic Press, 2011; Vol. *36*, pp. 35−102.

(12) Saatcioglu, E.; Ulag, S.; Sahin, A.; Yilmaz, B. K.; Ekren, N.; Inan, A. T.; Palaci, Y.; Ustundag, C. B.; Gunduz, O. Design and fabrication of electrospun polycaprolactone/chitosan scaffolds for ligament regeneration. *Eur. Polym. J.* **2021**, *148*, No. 110357.

(13) Chen, Y.; Miller, P. G.; Ding, X.; Stowell, C. E. T.; Kelly, K. M.; Wang, Y. Chelation Crosslinking of Biodegradable Elastomers. *Adv. Mater.* **2020**, *32*, 2003761.

(14) Hwang, S.-W.; Song, J.-K.; Huang, X.; Cheng, H.; Kang, S.-K.; Kim, B. H.; Kim, J.-H.; Yu, S.; Huang, Y.; Rogers, J. A. High-Performance Biodegradable/Transient Electronics on Biodegradable Polymers. *Adv. Mater.* **2014**, *26*, 3905−3911.

(15) Lee, H. J.; Jeong, B. ROS-Sensitive Degradable PEG−PCL−PEG Micellar Thermogel. *Small* **2020**, *16*, 1903045.

(16) Chang, S. H.; Lee, H. J.; Park, S.; Kim, Y.; Jeong, B. Fast Degradable Polycaprolactone for Drug Delivery. *Biomacromolecules* **2018**, *19*, 2302−2307.

(17) Mandolini, L.; Montaudo, G.; Scamporrino, E.; Roelens, S.; Vitalini, D. Organotin-mediated synthesis of macrocyclic tetraesters. A combined proton NMR spectroscopy, gel permeation chromatography, and fast atom bombardment mass spectrometry approach to complete product analysis. *Macromolecules* **1989**, *22*, 3275−3280.

(18) Gong, C.; Li, J.; Yi, C.; Qu, S. Catalytic Regulation of Oligomers in Polycaprolactone. *Mol. Catal.* **2021**, *508*, No. 111594.

(19) Michalicha, A.; Espona-Noguera, A.; Canal, C.; Budzyńska, B.; Pięt, M.; Przywara, S.; Pawelec, J.; Belcarz, A. Polycatecholamine and gentamicin as modifiers for antibacterial and blood-biocompatible polyester vascular prostheses. *Mater. Sci. Eng., C* **2022**, *133*, No. 112645.

(20) Zhang, J.; He, L.; Wei, G.; Jiang, X.; Fu, L.; Zhao, Y.; Zhang, L.; Yang, L.; Li, Y.; Wang, Y.; Mo, H.; Shen, J. Zwitterionic Polymer-Grafted Polylactic Acid Vascular Patches Based on a Decellularized Scaffold for Tissue Engineering. *ACS Biomater. Sci. Eng.* **2019**, *5*, 4366−4375.

(21) Nandakumar, V.; Suresh, G.; Chittaranjan, S.; Doble, M. Synthesis and Characterization of Hydrophilic High Glycolic Acid−Poly(dl-Lactic-co-Glycolic Acid)/ Polycaprolactam/Polyvinyl Alcohol Blends and Their Biomedical Application as a Ureteral Material. *Ind. Eng. Chem. Res.* **2013**, *52*, 751−760.

(22) Song, S.; Zhou, H.; Puzhitsky, M.; Zhang, Y.; Hicks, G.; Lu, Y.; Manners, I.; Winnik, M. A. Crystallization-Driven Self-Assembly of a Block Copolymer with Amphiphilic Pendant Groups. *Macromolecules* **2021**, *54*, 930−940.

(23) Bi, F.; Shao, J.; Xi, Z.; Zhao, L.; Liu, D. Synthesis and characterization of copolymers of poly(m-xylylene adipamide) and poly(ethylene terephthalate) oligomers by melt copolycondensation. *Chin. J. Chem. Eng.* **2016**, *24*, 1290−1297.

(24) Scherer, B.; Matysik, F.-M. Investigations of polymer samples of polyamide 11 concerning the content of monomer, oligomers, and the oxidation stabilizer Irganox 1098 by utilizing inverse gradient HPLC in combination with a triple detection system (diode array detection/mass spectrometry/charged aerosol detection). *Talanta Open* **2021**, *3*, No. 100023.

(25) Lam, C. X.; Hutmacher, D. W.; Schantz, J. T.; Woodruff, M. A.; Teoh, S. H. Evaluation of polycaprolactone scaffold degradation for 6 months in vitro and in vivo. *J. Biomed. Mater. Res., Part A* **2009**, *90A*, 906−919.

(26) Bartnikowski, M.; Dargaville, T. R.; Ivanovski, S.; Hutmacher, D. W. Degradation mechanisms of polycaprolactone in the context of chemistry, geometry and environment. *Prog. Polym. Sci.* **2019**, *96*, 1−20.

(27) Chlanda, A.; Kijeńska-Gawrońska, E.; Zdunek, J.; Swieszkowski, W. Internal nanocrystalline structure and stiffness alterations of electrospun polycaprolactone-based mats after six months of in vitro degradation. An atomic force microscopy assay. *J. Mech. Behav. Biomed. Mater.* **2020**, *101*, No. 103437.

(28) Rice, M. A.; Sanchez-Adams, J.; Anseth, K. S. Exogenously Triggered, Enzymatic Degradation of Photopolymerized Hydrogels with Polycaprolactone Subunits: Experimental Observation and Modeling of Mass Loss Behavior. *Biomacromolecules* **2006**, *7*, 1968−1975.

(29) Dewle, A.; Rakshasmare, P.; Srivastava, A. A Polycaprolactone (PCL)-Supported Electrocompacted Aligned Collagen Type-I Patch for Annulus Fibrosus Repair and Regeneration. *ACS Appl. Bio Mater.* **2021**, *4*, 1238−1251.

(30) Benedict, C. V.; Cameron, J. A.; Huang, S. J. Polycaprolactone degradation by mixed and pure cultures of bacteria and a yeast. *J. Appl. Polym. Sci.* **1983**, *28*, 335−342.

(31) Sundermann, J.; Oehmichen, S.; Sydow, S.; Burmeister, L.; Quaas, B.; Hänsch, R.; Rinas, U.; Hoffmann, A.; Menzel, H.; Bunjes, H. Varying the sustained release of BMP-2 from chitosan nanogel-functionalized polycaprolactone fiber mats by different polycaprolactone surface modifications. *J. Biomed. Mater. Res., Part A* **2021**, *109*, 600−614.

(32) Wang, D.; Wang, X.; Zhang, Z.; Wang, L.; Li, X.; Xu, Y.; Ren, C.; Li, Q.; Turng, L.-S. Programmed Release of Multimodal, Cross-Linked Vascular Endothelial Growth Factor and Heparin Layers on Electrospun Polycaprolactone Vascular Grafts. *ACS Appl. Mater. Interfaces* **2019**, *11*, 32533−32542.

(33) Bhatt, A.; Sakai, K.; Madhyastha, R.; Murayama, M.; Madhyastha, H.; Rath, S. N. Biosynthesis and characterization of nano magnetic hydroxyapatite (nMHAp): An accelerated approach using simulated body fluid for biomedical applications. *Ceram. Int.* **2020**, *46*, 27866−27876.

(34) Zhao, J.; Zhang, Z.; Yu, Z.; Yang, S.; Jiang, H. Synthesis of hydroxyapatite on thioglycolic acid-capped reduced graphene oxide/

https://doi.org/10.1021/acs.macromol.2c00275
Macromolecules 2022, 55, 5342−5352

silver nanoparticles: Effect of reaction condition in normal or pathological simulated body fluid. *Mater. Lett.* **2014**, *116*, 359−362.
(35) Eswaran, M.; Swamiappan, S.; Chokkiah, B.; Dhanusuraman, R.; Bharathkumar, S.; Ponnusamy, V. K. A green and economical approach to derive nanostructured hydroxyapatite from Garra mullya fish scale waste for biocompatible energy storage applications. *Mater. Lett.* **2021**, *302*, No. 130341.
(36) Laschke, M. W.; Witt, K.; Pohlemann, T.; Menger, M. D. Injectable nanocrystalline hydroxyapatite paste for bone substitution: In vivo analysis of biocompatibility and vascularization. *J. Biomed. Mater. Res., Part B* **2007**, *82B*, 494−505.
(37) Saha, N.; Dubey, A. K.; Basu, B. Cellular proliferation, cellular viability, and biocompatibility of HA-ZnO composites. *J. Biomed. Mater. Res., Part B* **2012**, *100B*, 256−264.
(38) Rahmati, M.; Mozafari, M. Protein adsorption on polymers. *Mater. Today Commun.* **2018**, *17*, 527−540.
(39) Chen, L.; Yan, C.; Zheng, Z. Functional polymer surfaces for controlling cell behaviors. *Mater. Today* **2018**, *21*, 38−59.
(40) Recek, N.; Jaganjac, M.; Kolar, M.; Milkovic, L.; Mozetič, M.; Stana-Kleinschek, K.; Vesel, A. Protein Adsorption on Various Plasma-Treated Polyethylene Terephthalate Substrates. *Molecules* **2013**, *18*, 12441−12463.
(41) Jiang, F.; Wang, S.; Liu, B.; Liu, J.; Wang, L.; Xiao, Y.; Xu, Y.; Liu, X. Insights into the Influence of CeO_2 Crystal Facet on CO_2 Hydrogenation to Methanol over Pd/CeO_2 Catalysts. *ACS Catal.* **2020**, *10*, 11493−11509.

https://doi.org/10.1021/acs.macromol.2c00275
Macromolecules 2022, 55, 5342−5352

9kkhW_Ery7Dm3ZL_9Cf3qfKAc485ysgAAALcwgbQGCSqGSIb3DQEHBqCBpjCBowIBADCBnQYJKoZIhvcNAQcBMB4GCWCGSAFlAwQBLjARBAzs0NCX5td_fH1q3Ru0CARCAcE-yGpm90Ex7FDZHAW4St38wFt0R6AQ82R4-6mX02sH6wkT-p3oS87qcUfRSRVgOfOk7L70372cKZUHIrVbX6aDYAJQ-